Chain polymers near an adsorbing surface

1994 J. Phys. A: Math. Gen. 27 4069

(http://iopscience.iop.org/0305-4470/27/12/015)

J. Phys. A: Math. Gen. 27 (1994) 4069–4081. Printed in the UK

Chain polymers near an adsorbing surface

Rainer Hegger and Peter Grassberger
Physics Department, University of Wuppertal, D-42097 Wuppertal, Germany

Received 18 January 1994

Abstract. We present improved estimates of critical exponents for 3D polymers near a plane adsorbing surface. The improvements were possible by simulating rather long chains (up to $N = 2000$) by means of a new algorithm. Apart from minor but significant adjustments in the location of the tricritical point and in the various γ-exponents, our main result is that the crossover exponent for critical adsorption is compatible with $\phi = \frac{1}{2}$. This is much lower than previous estimates and suggests that this exponent might be superuniversal.

1. Introduction

Polymers exhibit a rich variety of phase transitions and associated critical exponents. In the simplest case of a single chain in a good solvent, a homogeneous medium, and no interactions other than the excluded volume effect, polymers are modelled by self-avoiding walks (SAWs). As was shown by de Gennes [1], they correspond to the $n \to 0$ limit of an O(n) system. Other members of this family are the Ising model ($n = 1$), the XY model ($n = 2$) and the Heisenberg model ($n = 3$). These models were investigated intensively by the use of a variety of different methods, including mean-field approaches, perturbation theory, ϵ-expansions, transfer-matrix methods, exact enumerations and Monte Carlo simulations [2].

Other critical phenomena are obtained if one includes e.g. attractive self-interactions, long-range electrostatic repulsion, branched polymers, polymer networks, or inhomogeneous media.

The aspect which we are interested in here is provided by the presence of a plain surface to which one end of the polymer is attached (for a recent review, see [3]). Except for this complication, we consider the simplest case, i.e. a good solvent, no randomness of the medium, and a single unbranched polymer. We shall assume space to be three-dimensional throughout the paper, and model the polymer by a SAW on a simple cubic lattice.

The surface can be energetically neutral, presenting a purely geometrical restriction. But it can also be attractive for the polymer. In the latter case, the polymer will be adsorbed to the surface at low temperatures, while it is desorbed at high temperatures. Thus it is clear that there exists a phase transition from a high-temperature phase which is connected to the 3D bulk behaviour of SAWs, to a collapsed low-temperature phase of essentially 2D SAWs [4]. This is of course a sharp transition only in the limit of infinite chain length N, and is analogous to a tricritical point in a spin model [5, 6].

For the following it will be necessary to deal also with finite values of N or, equivalently, to consider a *grand canonical* ensemble of polymers instead of an ensemble with fixed chain length N. By 'grand canonical' we mean, of course, not that the number of chains is fluctuating, but the number of monomers, i.e. the chain length N. More precisely, let $C_{N,m}$

0305-4470/94/124069+13$19.50

be the number of configurations with length N, having m sites on the surface. Then our ensemble is defined by the partition function

$$Z^{(1)}(p,q) = \sum_{N,m} q^m p^N C_{N,m} = \sum_N p^N Z_N^{(1)}(q) . \tag{1}$$

Here,

$$q = \mathrm{e}^{-\beta\mathcal{E}} \tag{2}$$

is a Boltzmann factor associated with the energy $\mathcal{E}$ gained by a monomer (identified here with a lattice site†) if it is in contact with the surface ($\beta = 1/k_B T$; in the following we assume $\mathcal{E} = k_B = 1$). The variable p is a fugacity which we assume for simplicity to be independent of temperature. Finally,

$$Z_N^{(1)}(q) = \sum_m q^m C_{N,m} \tag{3}$$

is the 'canonical' partition sum at fixed N. The index '1' is to indicate that one end of the chain is attached to the surface.

Analogously, we can define $Z^{(11)}$ and $Z_N^{(11)}$ as sums over configurations where both ends are on the surface.

The phase diagram with the two fugacities p, pq as control parameters is shown in figure 1. For small p and q, long chains are exponentially suppressed, and the ensemble is dominated by short chains. Keeping p small but increasing q, we arrive at a point $q_0(p)$ where the average chain length diverges, but chains remain adsorbed to the surface‡.

Similarly, desorbed chains can grow indefinitely when $p \geqslant p_c$. Notice that p_c is independent of q, which means that p_c is just the critical value of p for SAWs in the bulk [4, 6] (= 0.2139... for a simple cubic lattice), and is the inverse of the *effective coordination number* μ, $p_c = 1/\mu$. The tricritical point $S = (p_c, q_c)$ where the two curves $q = q_0(p)$ and $p = p_c$ meet is analogous to the *special point* in magnetic transitions [6]. To its left, the half-line $p = p_c$ corresponds to an *ordinary transition* (polymer length diverges, no adsorption), to its right it is an *extraordinary transition* (length is already infinite, polymers desorb). Finally, it is clear that $Z_N^{(1)}(q)$ is analytic for all finite N, but develops a singularity at $q = q_c$ for $N \to \infty$.

2. Scaling laws

Let us now state the assumed scaling laws, and define the critical exponents [4].

Not only for $q < q_c$, but also at the transition point $q = q_c$, the radial extension of a chain with fixed large N (measured either via the end-to-end distance or the gyromagnetic ratio) is governed by the bulk exponent ν. Indeed, even at the transition point the chains are essentially isotropic, with the radius parallel and perpendicular to the surface both increasing as N^ν [6]. For $q > q_c$, $R_\perp \to$ constant and $R_\parallel \sim N^{\nu_2}$, where $\nu_2 = \frac{3}{4}$ is the two-dimensional exponent.

Below the transition point, the canonical partition sum scales as

$$Z_N^{(1)}(q) \sim \mu^N N^{\gamma_1 - 1} \qquad \text{for} \quad q < q_c . \tag{4}$$

† Notice that some authors [7, 8] prefer to identify monomers with bonds, which results in a different critical value of q.

‡ The partition sum for $q > q_0(p)$ is defined either by analytic continuation or by putting the whole system into a finite box and taking the limit of infinite volume at the end. The phase where a single polymer fills a whole macroscopic surface or volume is called the 'dense limit' [9, 10].

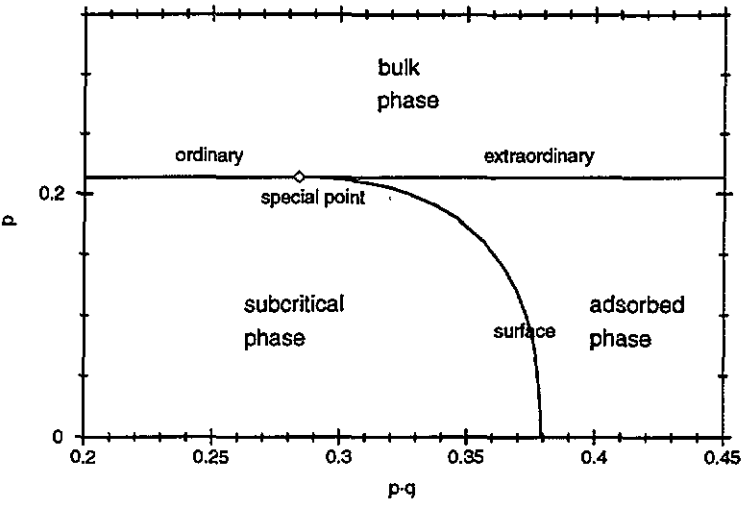

Figure 1. Phase diagram of a polymer attached at one end to a surface. The upper part is the bulk phase where a single polymer fills the bulk volume with finite density. The lower right part is the surface phase containing a long adsorbed polymer, and the lower left phase, finally, is the subcritical phase with only short chains. The horizontal line marks the *ordinary* (left) and *extraordinary* (right) transition, respectively, and the curved line marks the *surface transition*. The point where the two lines meet is the *special point*. The transitions were determined numerically, with error bars less than the line width. The method used to localize the surface transition will be discussed in section 4.2.

Notice that here the connectivity constant has its bulk value, while the exponent γ_1 is different from the analogous bulk exponent γ. This implies that $\mathcal{Z}(p, q)$ has a singularity $\propto (p_c - p)^{-\gamma_1}$ when $p \to p_c$ from below.

Above q_c, $Z_N^{(1)}(q)$ scales with the exponent of N in (4) assuming the 2D value $\gamma_{d=2} = \frac{43}{32}$ [2], and with a q-dependent connectivity 'constant'. At $q = q_c$, finally, $\mu = 1/p_c$ is again the bulk constant, but γ is to be replaced by a value γ_1^s.

An ansatz analogous to (4) can also be made for the canonical partition sum $Z_N^{(11)}$, with new exponents γ_{11}^s and γ_{11}, respectively.

For the grand canonical partition sum we make a scaling ansatz in terms of the deviations from the special point. As a function of p, $\mathcal{Z}^{(1)}(p, q)$ has a singularity at p_c for all q, but as a function of q it is analytic and non-vanishing for all $q \leqslant q_c$ (except when $p = p_c$). Thus a natural ansatz is

$$\mathcal{Z}^{(1)}(p, q) = (p_c - p)^{-\gamma_1^s} F\left(\frac{q - q_c}{(p_c - p)^{\phi}}\right) \tag{5}$$

where $F(z)$ is analytic and non-zero at $z = 0$, and ϕ is a new critical ('cross-over') exponent. The exponent of the prefactor in this ansatz is determined by the behaviour at $q = q_c$.

For the canonical partition sum, this corresponds to an ansatz

$$Z_N^{(1)}(q) = \mu^N N^{\gamma_1^s - 1} G((q - q_c)N^{\phi}) \tag{6}$$

where the scaling function $G(z)$ is related to $F(z)$ by a Laplace transform.

From this ansatz we find immediately that the surface transition (between the subcritical and the surface phase) is at $(q - q_c) \propto (p_c - p)^{\phi}$, i.e. at

$$q_0(p) = q_c + z_0(p_c - p)^{\phi} \tag{7}$$

where z_0 is a singularity of $F(z)$. Near z_0 we have

$$F(z) = \frac{\text{const}}{(z_0 - z)^{\gamma_{d=2}}} \tag{8}$$

since in this region the polymer is essentially adsorbed to the surface, and $Z^{(1)}(p, q)$ is essentially a partition sum of 2D polymers which diverges for $q \to q_0(p)$ with the exponent $-\gamma_{d=2}$.

Further scaling laws can be obtained as usual by differentiating the partition sums. The average energy in the canonical ensemble is given, e.g., by

$$E_N(T) = \frac{\mathcal{E}}{Z_N^{(1)}(q)} \sum_m m q^m C_{N,m} = \frac{\mathcal{E} q}{Z_N^{(1)}(q)} \frac{\partial Z_N^{(1)}(q)}{\partial q} \tag{9}$$

from which we find that the energy per monomer scales as [4]

$$E_N(T)/N \sim \begin{cases} [(T_c - T)N]^{-1} & T < T_c \\ N^{\phi-1} & T = T_c \\ (T - T_c)^{1/\phi - 1} & T > T_c \end{cases} . \tag{10}$$

Finally, we quote without derivation a relation between critical exponents [11, 12] which is expected to hold both at the ordinary and special transitions,

$$2\gamma_1 - \gamma - \gamma_{11} = \nu . \tag{11}$$

3. The algorithm

In the following we shall use Monte Carlo simulations on a simple cubic lattice, in order to test the above scaling relations and to estimate the critical exponents. The surface is located at $z = 0$. The algorithm we use is similar to that presented in [13, 14], but with a slight but important improvement. This algorithm is very effective (independently of q), it allows one to generate samples with any desired bias, and it is very easy to implement.

The structure of the algorithm is recursive. Its main part is a subroutine STEP with arguments (x, N) which sets the $(N$th) monomer at a site x adjacent to the end of an $(N-1)$-step chain, and marks this sites as occupied. Then it selects a random neighbour y of x and tests whether this site is still free (for optimal efficiency, we should avoid immediate reversals. Thus, y is chosen from among $\mathcal{N}-1$ neighbours, where $\mathcal{N} = 6$ is the coordination number of the lattice). If it is free, it makes $\mathcal{P} > 1$ calls to itself *on average*, with new arguments $(y, N+1)$. Here, $\mathcal{P} > 1$ is a positive number which is arbitrary in principle, though the efficiency of the algorithm depends strongly on a good choice for it. More precisely, if $\mathcal{P} = k + r$ with k an integer and $0 \leqslant r < 1$, we first call STEP k times, then draw a random number ξ uniformly in $[0, 1]$, and call STEP again iff $\xi < r$†. After that, the site x is marked as free again, and the subroutine is left.

Notice that this would be just naive sampling, if $\mathcal{P} = 1$ and if STEP would always call itself exactly once (provided the new site is free). By choosing $\mathcal{P} > 1$, our algorithm is essentially an enrichment method [15], but with a very different and much more efficient data structure than in the original implementation of [16]. We could speed up the algorithm slightly by hand-coding the recursion in order to avoid the recursive subroutine call, but

† This is the main difference with respect to the version of the algorithm presented in [13]. There, it was proposed to make $\mathcal{P}$ steps on average by trying not *one single* neighbour, but by making independent trials to step towards *each* of the neighbours of x. This would create much bigger fluctuations in the number of steps actually performed, making the algorithm thereby less efficient.

the difference in speed was sufficiently small that the additional effort (and the chance of making errors!) did not seem worthwhile.

The flexibility of this algorithm results from the fact that $\mathcal{P}$ need not be a constant, but can be virtually any function of N, y, and of the neighbouring pattern of occupation.

To obtain a grand canonical ensemble cut off at $N = N_{\max}$, with a surface at $z = 0$, we just have to take

$$\mathcal{P} = \mathcal{P}_{\mathrm{gc}}(z, N) = \begin{cases} (\mathcal{N}-1)p & z > 0 \quad \text{and} \quad N \leqslant N_{\max} \\ (\mathcal{N}-1)qp & z = 0 \quad \text{and} \quad N \leqslant N_{\max} \\ 0 & z < 0 \quad \text{or} \quad N > N_{\max} \end{cases} \tag{12}$$

where $\mathcal{N}$ is the coordination number of the lattice.

As shown in [14], efficiency of this algorithm is slightly improved by replacing the grand canonical ensemble by an ensemble in which all chain lengths are represented by roughly the same number of walks. This can be achieved, without changing the absorption strength of the surface, by multiplying $\mathcal{P}_{\mathrm{gc}}(z, N)$ by $(1 + 1/N)^{1-\gamma_1}$, thus obtaining

$$\mathcal{P}_{\mathrm{opt}}(z, N) = \mathcal{P}_{\mathrm{gc}}(z, N)(1 + 1/N)^{1-\gamma_1} . \tag{13}$$

Here, γ_1 has of course to be replaced by γ_1^s when studying the special point. We should however point out that it is not necesaary that γ_1 is known very precisely *a priori*. First of all, the improvement obtained by replacing $\mathcal{P}_{\mathrm{gc}}(z, N)$ in favour of $\mathcal{P}_{\mathrm{opt}}(z, N)$ is not very big, and secondly, a rough and sufficient estimate can be obtained in auxiliary runs with low statistics.

Let $n(N)$ be the number of N-step chains in the sample. The canonical partition sum is then estimated simply by

$$Z_N^{(1)}(q) = n(N) \Big/ \left[n(0) p^N \prod_{N'=1}^{N} (1 + 1/N')^{1-\gamma_1} \right] . \tag{14}$$

As in all implementations of the enrichment method, the chains of the so-constructed ensemble are statistically not independent [15]. This is often considered to be its main weakness, but it is not as bad as usually claimed. Like the algorithms of [17, 18], the algorithm essentially performs a random walk in the chain length N with reflecting boundaries at $N = 0$ and $N = N_{\max}$ [18], and two chains are independent only if N had vanished in between (i.e. a completely new chain had been started). Thus the number of independent chains of length N can be estimated by counting how often the length had oscillated between 0 and N. The set of all chains between two consecutive returns to $N = 0$ (i.e. to the main routine) will be called a 'tour'.

As suggested by the random-walk picture, the number of steps needed to obtain a tour with at least one chain of length $\geqslant N$ increases quadratically [18] as N^2/D, where D is an effective diffusion constant. We found that $D \approx 15$. This is in contrast to the previous algorithms [17, 18] which all have $D \approx 1$. In particular, the above value of D is about a factor 6.5 larger than for the version of [13], and explains its efficiency.

An *a priori* estimate for D is provided by the following argument. Assume that $\mathcal{P}$ is chosen according to (12) with $p = p_c$, and $\epsilon = \mathcal{P} - 1$ is small (which is true for high dimensions). Then the random walk in N is unbiased, and a back step is only needed when the walker hits an occupied site. The chance for this is $\approx \epsilon$. This means that in average $1/\epsilon$ forward steps are made between two back steps, each back step reducing N by roughly $1/\epsilon$. This leads to

$$D \sim 1/\epsilon . \tag{15}$$

We also made simulations on the square lattice ($\epsilon = 0.137$) and on the 4D hypercubic lattice ($\epsilon = 0.0334$), and verified (15).

Since the probability $P_{\text{success},N}$ ($\approx D/N$ for the 'optimal' choice of $\mathcal{P}$) for a tour to be 'successful' in reaching length N is $\ll 1$ for large N, the number $k(N)$ of successful tours has a relative RMS error $1/\sqrt{P_{\text{success},N}}$. This sets also a lower limit to the relative error of the number of generated chains of length N. We found numerically that the actual variance of the latter is about twice as large, $\Delta n(N)/n(N) \approx 1.4/\sqrt{k(N)}$. The relative error of the end-to-end distance R_N (both perpendicular and parallel to the surface) was also inversely proportional to the number of successful tours, $\Delta R_{\perp N}/R_{\perp N} \approx 0.4/\sqrt{k(N)}$ and $\Delta R_{\parallel N}/R_{\parallel N} \approx 0.6/\sqrt{k(N)}$, respectively. Similar error estimates were found for the other observables.

Our total sample consists of seven subsamples taken at different values of q. Each subsample consists of $\approx 2 \times 10^7$ tours which contain $\approx 150\,000$ 'successful' tours which reached $N_{\max} = 2000$. Since we used the optimal choice $\mathcal{P}_{\text{opt}}$, the total number of chains of length $N_{\max}$ was also $\approx 2 \times 10^7$ for each subsample, out of which 150 000 are strictly independent. This might not sound very efficient, but it leads to very small statistical errors, as can be checked by means of the above estimates.

Altogether, creating this sample—which is at least one order of magnitude larger than all previous samples—took about 500 h CPU time on DEC 3000/300 AXP workstations.

4. Results

4.1. The ordinary transition

We begin with the ordinary transition, i.e. the transition from the *subcritical* to the bulk phase. In particular, we used $q = 1$, in which case the surface merely plays the role of a geometrical restriction without any further energetic effects.

The canonical partition sums are computed from (14). Since we must expect corrections to the scaling law (4) from confluent singularities [6, 3],

$$p_c^N Z_N^{(1)}(q) = (N+b)^{\gamma_1 - 1}\left(1 + \frac{a}{N^\Delta} + \cdots\right) \tag{16}$$

with unknown constants $a, b, \Delta \ldots$, we computed effective exponents

$$\gamma_{1,\text{eff}}^{(N)} = 1 + \frac{\log\left[p_c^N Z_{2N}^{(1)}(q)/Z_N^{(1)}(q)\right]}{\log[(2N+b)/(N+b)]}. \tag{17}$$

For $N \to \infty$ they should converge to γ_1 as

$$\gamma_{1,\text{eff}}^{(N)} = \gamma_1 + \frac{a'}{N^\Delta} + \cdots. \tag{18}$$

In equation (17) it is crucial to take a precise value of p_c, since an error Δp_c in p_c gives rise to an error $N\Delta p_c/(p \log 2)$ in $\gamma_{1,\text{eff}}^{(N)}$.

Values obtained with three different values of p_c (0.213 492 4, 0.213 490 8 and 0.213 489 2) are plotted in figure 2 against $1/N^{0.75}$. It it obvious from these data that the estimate of p_c from [14] is somewhat too large. We can definitely exclude the even larger value $p_c = 0.213\,498\,7$ of [19] (though these authors quoted very small error bars) and the similar value of [20]. From our data we propose

$$p_c = 0.213\,490\,8 \pm 0.000\,000\,5. \tag{19}$$

The parameter b in (17) was set to $b = 0$. The exponent of N on the abscissa of figure 2 was chosen such that the curve for $p = p_c$ is linear, and gives us $\Delta = 0.75$. We had to use $\Delta < 1$ in order to ensure linearity, but there was no need for $b \neq 0$.

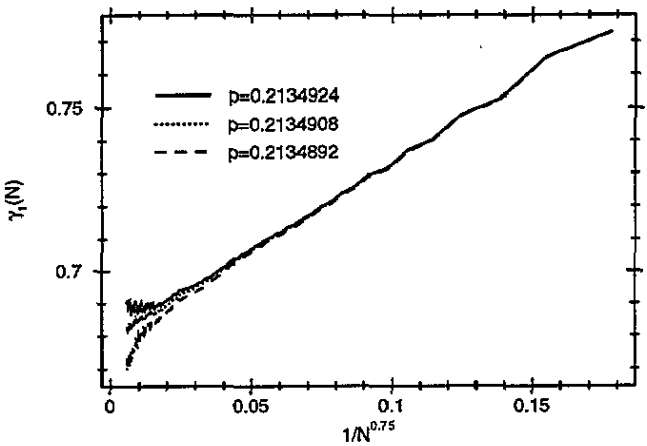

Figure 2. N-dependent estimates for the exponent γ_1, obtained by taking for p_c the values 0.213 489 2, 0.213 490 8 and 0.213 492 4. The parameter b in (17) was set to 0. On the horizontal axis we plotted $1/N^{0.75}$, which was necessary to obtain linear behaviour.

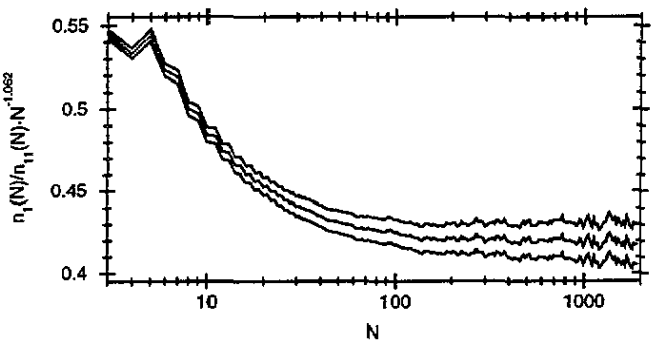

Figure 3. The product $Z_N^{(1)}/Z_N^{(11)} \times N^{-x}$, with three different values of x (1.058, 1.062 and 1.066, starting from above). These powers were chosen such that the curves become roughly horizontal for large N, and equal to $\gamma_1 - \gamma_{11}$ within the error bars. To reduce statistical fluctuations, data are averaged over bins with width $\Delta N/N = 0.02$.

When performing the same analysis for the exponent γ_{11}, we find much larger statistical fluctuations (since the chance that a long chain will have its end on the surface is very small). To estimate γ_{11}, we use the ratio $Z_N^{(1)}/Z_N^{(11)}$ which is independent of p_c. An additional factor N^{-x} is multiplied such that the resulting expression $Z_N^{(1)}/Z_N^{(11)}N^{-x}$ is roughly constant for large N (see figure 3).

Our final results for the exponents are thus

$$\gamma_1 = 0.679 \pm 0.002 \qquad \gamma_{11} = -0.383 \pm 0.005\,. \tag{20}$$

These values are in good agreement with the (rather imprecise) results from exact enumerations [3] and from the ϵ-expansion [5]. Our γ_{11} is also in agreement with that from

the best previous simulations [20], while our γ_1 is somewhat lower than the value from [20]. But due to the better statistics, the accuracy of our estimates is roughly a factor of two better. To test the scaling relation (11), we use the estimates $\gamma = 1.1608 \pm 0.0003$ and $\nu = 0.585 \pm 0.0015$ of [14], and get

$$\gamma - 2\gamma_1 + \gamma_{11} + \nu = 0.005 \pm 0.006 . \tag{21}$$

We mention finally that our critical exponents violate the Bray–Moore conjecture $\gamma_{11} = \nu - 1$ [21] which is also violated in $d = 2$ [24] and in second order of $\epsilon = 4 - d$.

4.2. The special point

In contrast to p_c, the value of q_c is not known with high precision from previous analyses. From [20] and from figure 1 we know just that q_c lies in the vicinity of 1.33.

Also, it is less trivial to compute observables at different values of q from raw data which were taken at a different q. This could be done straightforwardly if one could store all joint distributions. For our chain lengths this was not feasible. Approximate readjustments of q could be made if one assumes linearity of the observables in q, since the derivatives can be calculated via second moments involving the relevant observable and the number m of surface contacts. We preferred not to do this either, but to make independent runs at different values of q close to q_c.

We thus performed runs with 6 different values of q between $q = 1.3297$ and $q = 1.3331$. Their results are shown in figures 4 to 9.

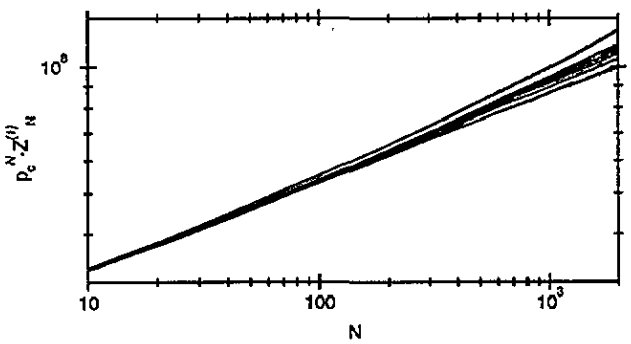

Figure 4. $p_c^N Z_N^{(1)}(q)$ for the six different q-values (starting with the lowest curve) 1.3297, 1.3305, 1.3310, 1.3314, 1.3320 and 1.3331. p_c was set to 0.213 490 8, the value found at the ordinary transition.

In figure 4 we show $p_c^N Z_N^{(1)}(q)$ with $p_c = 0.213\,490\,8$, and effective exponents for γ_1^s computed from these data according to (17) in figure 5. The average energy (more precisely $E_N(q)\sqrt{N}$) and estimates computed therefrom for the exponent ϕ are shown in figures 6 and 7. The ratios $Z_N^{(1)}/Z_N^{(11)} \times N^{-0.516}$ are shown in figure 8. We do not show effective exponents for them since this plot would be too noisy. Finally, in figure 9 we show effective exponents obtained from the end-to-end distances. In contrast to the previous plots, there we also show data for $q = 1$, and only plot results for three values of q near q_c.

All data displayed in figures 4–9 show substantial corrections to scaling. It would thus be very dangerous to determine q_c from only one of these plots, and to use it later in determining critical exponents, as it was done, for example, in [20]. For instance, the data for $Z_N^{(1)}$ (figure 4) seem to be straightest for the smallest value of q (= 1.3297) (unless

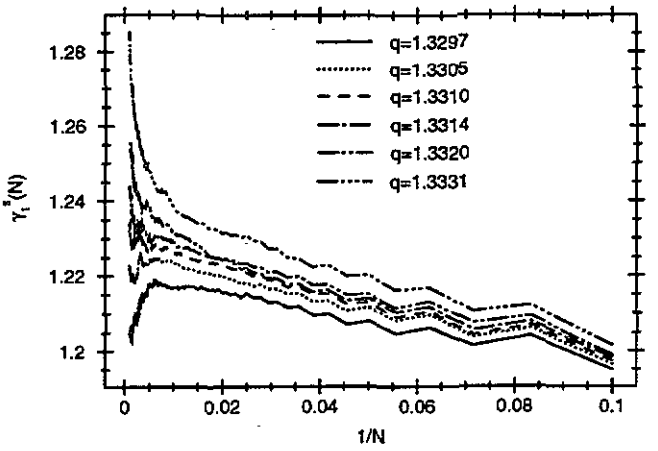

Figure 5. N-dependent estimates for the exponent γ_1^s, using the data from figure 4 and an equation analogous to (17). Parameters are $b = 0$ and $\Delta = 1$, i.e. the data are plotted against $1/N$. The six curves correspond to the same values of q as in figure 4.

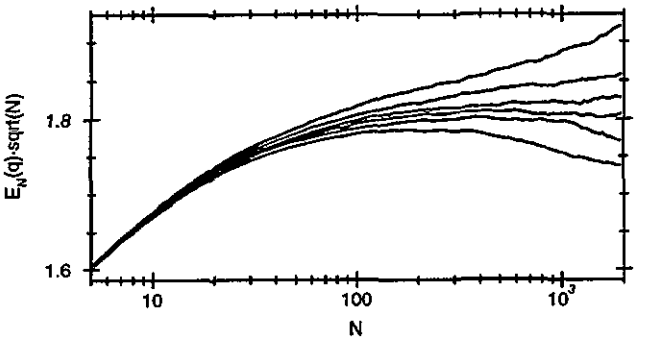

Figure 6. $E_N(q) \times \sqrt{N}$ for the same six values of q as in figure 4. The lowest curve corresponds to the smallest q. As in figure 3 we averaged over bins with $\Delta N/N = 0.02$.

we accept a completely unrealistic value for p_c), and it is only due to our high statistics and large range of N that we see from figure 5 that indeed this value of q is definitely subcritical. In contrast, the energies shown in figure 6 would have suggested a too large value of q if we had simply fitted a straight line without allowing for corrections to scaling.

In order to estimate q_c, we thus do not rely exclusively on any one of these distributions, but look for a good compromise. Such a compromise does indeed exist (which is again a check for our estimate for p_c), and our best estimate is

$$q_c = 1.3310 \pm 0.0003\,. \tag{22}$$

The corresponding transition temperature is

$$T_s = 1/\log q_c = 3.497 \pm 0.003\,. \tag{23}$$

This differs considerably from the result $T_s = 3.436 \pm 0.012$ ($q_c = 1.3378 \pm 0.0013$) of the best previous Monte Carlo simulations [20] which used much shorter chains (mostly $N_{max} = 350$, compared to our $N_{max} = 2000$). Thus it seems very likely that the results of [20] are strongly affected by scaling corrections.

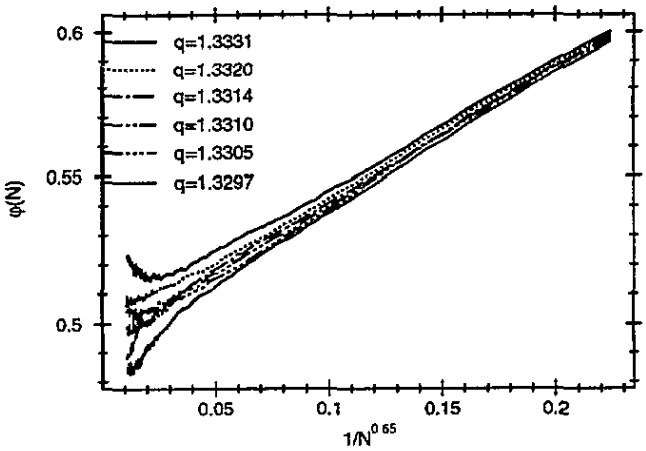

Figure 7. Similar to figure 2, but for the exponent ϕ belonging to the mean energy per chain, and using $b = -0.8$ and $\Delta = 0.65$.

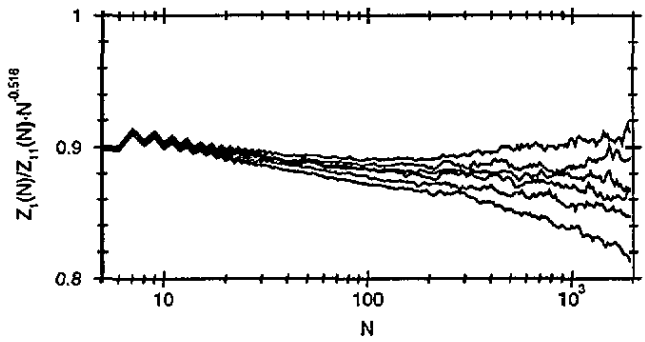

Figure 8. The ratio $Z_N^{(I)}/Z_N^{(II)} \times N^{-0.516}$ for the six different values of q. The upper curve corresponds to the smallest q. Again we averaged over intervals $\Delta N/N = 0.02$.

With this estimate of q_c, the critical exponents can be read off directly from figures 5, 7, and 8. From figure 5 we obtain

$$\gamma_1^s = 1.230 \pm 0.002 \tag{24}$$

from figure 7 we find

$$\phi = 0.496 \pm 0.004 \tag{25}$$

and from figure 8 we can read off $\gamma_1^s - \gamma_{11}^s = 0.516 \pm 0.006$, leading to

$$\gamma_{11}^s = 0.714 \pm 0.006\,. \tag{26}$$

The end-to-end distances (figure 9) are sufficiently precise to give an independent check for q_c (in particular, the large estimate of q_c from [20] is excluded), and to test the internal consistency of our data. But they are not precise enough to improve the previous estimate for the exponent ν [14] which was mainly based on the very high statistics simulations of [22].

A final independent estimate of ϕ (and check of q_c) results from analysing the shape of the surface transition curve in figure 1 (equation (7)). This curve was obtained numerically

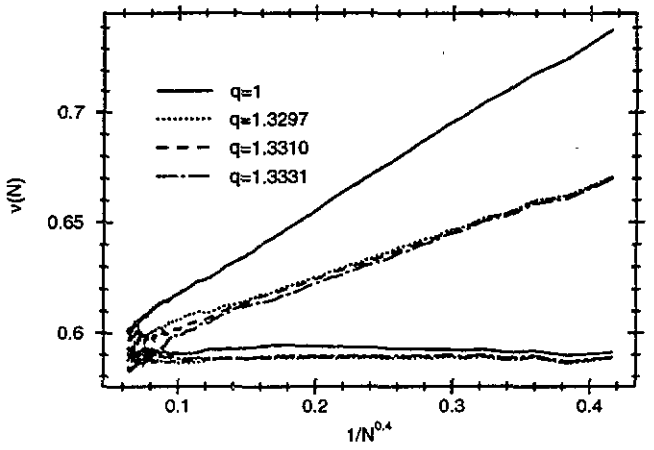

Figure 9. Estimates for the exponent ν obtained with (17). In contrast to the preceding figures, *the curves correspond to* $q = 1$, *1.3297, 1.3310 and 1.3331. The upper set of curves is obtained* from $R_\perp$, the lower from $R_\parallel$. With increasing q, $\nu_{\rm eff}$ decreases for the former, while no clear systematics is seen for the latter, except for $q > q_c$. The parameter b is 0. Data are plotted against $1/N^{0.4}$.

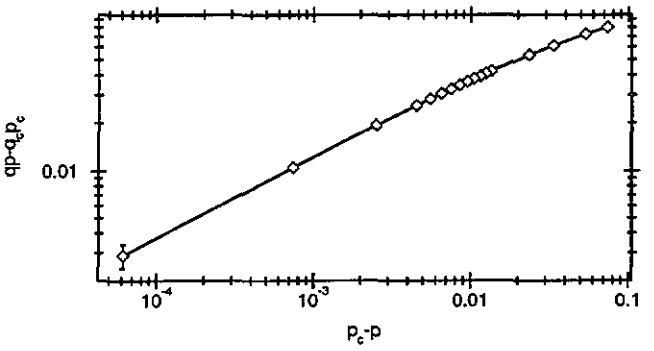

Figure 10. Log–log plot of $p_c - p$ against $q_0(p)p - q_c p_c$. The errors include both statistical errors of the the estimation of $q_0(p)$, and systematic errors due to the uncertainties in p_c and q_c.

by demanding that $p^N Z_N^{(1)}(q)$ scales as $N^{\gamma_d=2}$ in the range $10 \leqslant N \leqslant N_{\max}$. This is of course only correct if the value of p is far enough from p_c, since we would otherwise be in the cross-over region. For some values of p close to p_c we used smaller fitting intervals (increasing the lower bound on N), but this then gives rise to very large statistical errors. The results, plotted on a log–log plot of $p_c - p$ against $q_0(p)p - q_c p_c$ and using the estimated values of p_c and q_c, are shown in figure 10. We see approximately a straight line, giving an exponent $\phi = 0.5 \pm 0.03$ which agrees with (25), but with much larger error bars.

All our exponents are substantially different from the best previous estimates. In particular, our γ exponents are considerably smaller than those given in [20] ($\gamma_1^s = 1.304 \pm 0.006$, $\gamma_{11}^s = 0.806 \pm 0.015$) and in [4] ($\gamma_1^s = 1.44 \pm 0.03$). The value of γ_1^s is also smaller than that obtained from exact enumerations of short chains in [23]. They are in good agreement with those obtained from second-order ϵ-expansion [5], $\gamma_1^s \simeq 1.24$ and $\gamma_{11}^s \simeq 0.72$. The latter should, however, not be taken too seriously since the same order of

the ϵ-expansion gives the very wrong prediction $\phi = 0.67$. Finally, our gamma exponents satisfy the Barber scaling relation (11),

$$\gamma - 2\gamma_1^s + \gamma_{11}^s + \nu = -0.0002 \pm 0.007\,. \tag{27}$$

Our value of ϕ is also much lower than previous estimates. In particular, reference [20] quoted 0.530 ± 0.007, while [4] had obtained 0.58 ± 0.03. The origin of these discrepancies is obviously the large corrections to scaling seen in figure 6 which at the same time lead to overestimations of ϕ and of q_c. Our result suggests that indeed $\phi = \frac{1}{2}$, as for $d = 2$ and $d = 4$ [25]. Since, moreover, $\phi = \frac{1}{2}$ holds exactly for lattice animals (branched polymers) in $d = 3$ [26], we have the interesting possibility that ϕ is superuniversal. We should however mention that a numerical study of branched polymers in $d = 3$ [27] gave $\phi = 0.70 \pm 0.06$, and that the ϵ-expansion predicts that $\phi \neq \frac{1}{2}$ in $d = 4 - \epsilon$ [5]. Obviously this problem deserves further attention.

5. Discussion

We have applied a new Monte Carlo algorithm to the problem of polymers near an adsorbing surface. It is not quite as fast as the pivot algorithm [28] in cases where the latter is efficient. But our algorithm has the advantages that it is fairly simple, fast, and is not slowed down in complex geometries or in the presence of interactions, where other algorithms become extremely inefficient.

We compared our results mainly to previous simulations [20] which were done with an algorithm which is very efficient for medium-long chains, but whose efficiency decreases exponentially with chain length. The fact that we could simulate much longer chains (up to $N = 2000$) with very high statistics allowed us to see important corrections to scaling which went unseen in previous analyses. This concerns mainly the tricritical ('special') point, while our results for the ordinary transition agree essentially with values found in the literature.

Taking these corrections to scaling into account, we find that the exponents γ_1^s and γ_{11}^s and the cross-over exponent ϕ are all much smaller than according to previous estimates. The most interesting result is that ϕ is consistent with $\frac{1}{2}$ (our best estimate is 0.496 ± 0.005), suggesting that $\phi = \frac{1}{2}$ is indeed a superuniversal result for critically adsorbed polymers in all dimensions between two and four.

Apart from this, our results are in reasonable agreement with older results for polymers in the bulk. This concerns mainly the values for p_c and for ν. It shows that our method has indeed no bias, and is very efficient. Applications to polymer adsorption in $d = 2$, to theta polymers in $d = 2$ and $d = 3$, to polymer solutions in the dense limit and to SAWs in $d = 4$ will be presented elsewhere.

References

[1] de Gennes P 1979 *Scaling Concepts in Polymer Physics* (Ithaca, NY: Cornell University Press)
[2] de Cloizeaux J and Jannink G 1990 *Polymers in Solution* (Oxford: Clarendon)
[3] De' Bell K and Lookman T 1993 *Rev. Mod. Phys.* 65 87
[4] Eisenriegler E, Kremer K and Binder K 1982 *J. Chem. Phys.* 77 6296
[5] Diehl H W and Dietrich S 1981 *Phys. Rev.* B 24 2878
[6] Diehl H W 1986 *Phase Transitions and Critical Phenomena* vol 10, ed C Domb and J L Lebowitz (New York: Academic)
[7] Ishinabe T 1982 *J. Chem. Phys.* 76 5589; 77 3171; 1984 *J. Chem. Phys.* 80 1318
[8] Foster D P, Orlandini E and Tesi M C 1992 *J. Phys. A: Math. Gen.* 25 L1211

[9] Duplantier B and Saleur H 1987 *Nucl. Phys.* B **290** 291
[10] Schäfer L 1990 *Nucl. Phys.* B **344** 596
[11] Barber M N 1973 *Phys. Rev.* B **8** 407
[12] Barber M N, Guttmann A J, Middlemiss K M, Torrie G M and Whittington S G 1978 *J. Phys. A: Math. Gen.* **11** 1833
[13] Grassberger P 1993 *J. Phys. A: Math. Gen.* **26** 1023
[14] Grassberger P 1993 *J. Phys. A: Math. Gen.* **26** 2769
[15] Kremer K and Binder K 1988 *Comput. Phys. Rep.* **7** 259–310
[16] Wall F T and Erpenbeck J J 1959 *J. Chem. Phys.* **30** 634, 637
[17] Redner S and Reynolds P J 1981 *J. Phys. A: Math. Gen.* **14** 2679
[18] Beretti A and Sokal A D 1985 *J. Stat. Phys.* **40** 483
[19] MacDonald D, Hunter D L, Kelly K and Jan N 1992 *J. Phys. A: Math. Gen.* **25** 1429
[20] Meirovitch H and Livne S 1988 *J. Chem. Phys.* **88** 4507
[21] Bray A J and Moore M A 1977 *J. Phys. A: Math. Gen.* **10** 1927
[22] Caracciolo S, Ferraro G and Pelisetto A 1991 *J. Phys.* **24** 3625
[23] Zhao D, Lookman T and De'Bell K 1990 *Phys. Rev.* A **42** 4591
[24] Guim I and Burkhardt T W 1989 *J. Phys. A: Math. Gen.* **22** 1131
[25] Burkhardt T W, Eisenriegler E and Guim I 1989 *Nucl. Phys.* B **316** 559
[26] Janssen H K and Lyssy A 1992 *J. Phys. A: Math. Gen.* **25** L679
[27] Orlandini E *et al* 1993 *Phys. Rev.* E **48** R4203
[28] Madras N and Sokal A D 1988 *J. Stat. Phys.* **50** 109